



# Macromolecular Proton Fraction as a Myelin Biomarker: Principles, Validation, and Applications

Alena A. Kisel<sup>1,2</sup>, Anna V. Naumova<sup>1</sup> and Vasily L. Yarnykh<sup>1,2\*</sup>

<sup>1</sup> Department of Radiology, University of Washington, Seattle, WA, United States, <sup>2</sup> Laboratory of Neurobiology, Tomsk State University, Tomsk, Russia

Macromolecular proton fraction (MPF) is a quantitative MRI parameter describing the magnetization transfer (MT) effect and defined as a relative amount of protons bound to biological macromolecules with restricted molecular motion, which participate in magnetic cross-relaxation with water protons. MPF attracted significant interest during past decade as a biomarker of myelin. The purpose of this mini review is to provide a brief but comprehensive summary of MPF mapping methods, histological validation studies, and MPF applications in neuroscience. Technically, MPF maps can be obtained using a variety of quantitative MT methods. Some of them enable clinically reasonable scan time and resolution. Recent studies demonstrated the feasibility of MPF mapping using standard clinical MRI pulse sequences, thus substantially enhancing the method availability. A number of studies in animal models demonstrated strong correlations between MPF and histological markers of myelin with a minor influence of potential confounders. Histological studies validated the capability of MPF to monitor both demyelination and re-myelination. Clinical applications of MPF have been mainly focused on multiple sclerosis where this method provided new insights into both white and gray matter pathology. Besides, several studies used MPF to investigate myelin role in other neurological and psychiatric conditions. Another promising area of MPF applications is the brain development studies. MPF demonstrated the capabilities to quantitatively characterize the earliest stage of myelination during prenatal brain maturation and protracted myelin development in adolescence. In summary, MPF mapping provides a technically mature and comprehensively validated myelin imaging technology for various preclinical and clinical neuroscience applications.

**Keywords:** macromolecular proton fraction (MPF), myelin, magnetization transfer (MT), central nervous system, brain, spinal cord, MRI, quantitative imaging

## OPEN ACCESS

### Edited by:

Jiazheng Wang,  
Philips Research, Netherlands

### Reviewed by:

Silvia De Santis,  
Cardiff University, United Kingdom

### \*Correspondence:

Vasily L. Yarnykh  
yarnykh@uw.edu

### Specialty section:

This article was submitted to  
Brain Imaging Methods,  
a section of the journal  
Frontiers in Neuroscience

**Received:** 22 November 2021

**Accepted:** 17 January 2022

**Published:** 09 February 2022

### Citation:

Kisel AA, Naumova AV and  
Yarnykh VL (2022) Macromolecular  
Proton Fraction as a Myelin  
Biomarker: Principles, Validation, and  
Applications.  
*Front. Neurosci.* 16:819912.  
doi: 10.3389/fnins.2022.819912

## INTRODUCTION

Investigation of myelin damage, repair, and development in the central nervous system (CNS) for the understanding of pathological mechanisms and treatment monitoring in various neurological and psychiatric conditions using non-invasive imaging methods attracted substantial attention over past two decades (Heath et al., 2018; Piredda et al., 2021). Myelin has been recognized as a key source of brain tissue contrast in MRI due to its strong effect on the nuclear magnetic

resonance relaxation times  $T_1$  and  $T_2$  (Piredda et al., 2021). However, conventional MRI does not allow quantitation of the myelin content changes and lacks specificity to myelin. Recent progress in quantitative MRI methods resulted in the development of several specialized techniques with improved specificity to myelin, which potentially can be used as sources of myelin biomarkers. The underlying biophysical tissue properties affected by myelin include single- or multi-component relaxation, magnetization transfer, anisotropic diffusion, and magnetic susceptibility (Heath et al., 2018; Piredda et al., 2021). Extensive overview of the current myelin imaging methods can be found in recent reviews (Heath et al., 2018; Piredda et al., 2021). Several recently published meta-analyses (Mancini et al., 2020; Lazari and Lipp, 2021; van der Weijden et al., 2021) compared multiple histological validation studies of prospective myelin imaging biomarkers. While there is no evidence of a superiority of any single myelin imaging method to date, the above studies consistently identified the macromolecular proton fraction (MPF) among the parameters enabling the strongest correlations with myelin histology.

MPF is a parameter describing the magnetization transfer (MT) effect and defined as a relative amount of protons bound to biological macromolecules with restricted molecular motion, which participate in magnetic cross-relaxation with free water protons (Yarnykh, 2012). MPF offers several important advantages as a myelin biomarker. Particularly, MPF has fewer physiological confounders as compared to myelin measures based on diffusion, relaxation, and susceptibility. Diffusion indexes associated with myelination, such as radial diffusivity and fractional anisotropy (Song et al., 2002), are affected by microstructural tissue organization and spatial orientation of myelinated fibers (Wheeler-Kingshott and Cercignani, 2009), whereas MPF is independent of these factors (Underhill et al., 2009; Stikov et al., 2011). Relaxation times  $T_1$ ,  $T_2$ , and  $T_2^*$  and magnetic susceptibility in neural tissues are mainly determined by both myelination and concentration of iron (Stüber et al., 2014; Duyn and Schenck, 2017). As a consequence, a popular myelin biomarker, myelin water fraction measured from multi-component relaxation analysis (MacKay et al., 1994; Deoni et al., 2008; Hwang et al., 2010) is also influenced by the iron content (Birkl et al., 2019). In contrast, MPF is not affected by iron or other paramagnetic ions in tissues (Li et al., 2016; Trujillo et al., 2017a; Yarnykh et al., 2018a). MPF is also independent of magnetic field strength. *In vivo* MPF measurements in the brain white matter (WM) and gray matter (GM) appeared quantitatively consistent in a wide range of magnetic fields from 0.5 T (Anisimov et al., 2020) to 11.7 T (Naumova et al., 2017). Therefore, MPF provides an attractive approach as a uniform quantitative scale of myelin measurements across a variety of human and animal MRI platforms. Finally, MPF maps can be obtained using routine MRI equipment without modification of original manufacturers' pulse sequences (Yarnykh et al., 2018b; Korostyshevskaya et al., 2019; Smirnova et al., 2021) thus facilitating clinical translation of this technology.

While MPF mapping has been in use for almost 20 years, the current literature lacks a review specifically focused on MPF as a myelin biomarker. In this review, we sought to provide

a brief but comprehensive summary of existing MPF mapping techniques, histological validation studies, and MPF applications in neuroscience. The review is based on PubMed literature search including synonyms of MPF (such as "bound pool fraction," "bound proton fraction," "semisolid pool fraction," "semisolid proton fraction," and "bound water fraction") and a similar quantity, pool size ratio (PSR) (Gochberg and Gore, 2003) related to MPF as  $PSR = MPF/(1-MPF)$ . The term MPF is uniformly used below, although different notations can be found in original publications. The search methodology is detailed in Supplementary Material.

## LITERATURE REVIEW

### Macromolecular Proton Fraction Mapping Methods

The group of methods allowing reconstruction of MPF maps alone or in combination with other MT parametric maps is commonly referred to as quantitative MT (qMT). The two-pool model of MT (Morrison and Henkelman, 1995) provides a general theoretical framework for all qMT techniques. Within this model, tissue is represented by two proton magnetization reservoirs (free water and macromolecular pool), where the process of magnetization exchange is described by the cross-relaxation rate constant and MPF. Each pool has own transverse and longitudinal relaxation times. We recommend reviews (Henkelman et al., 2001; Sled, 2018) for more details of biophysics of the MT effect. The model parameters can be estimated using the two basic strategies: analysis of a signal behavior in response to off-resonance radiofrequency (RF) saturation with variable offset frequency and power (Z-spectroscopy) and analysis of temporal signal evolution after initial semi-selective perturbation of either water or macromolecular magnetization, which is described by the bi-exponential function (cross-relaxometry). In the contemporary formulation, the two-pool model for tissues includes the super Lorentzian spectral line-shape of the macromolecular pool and Lorentzian line-shape of the free water pool (Morrison and Henkelman, 1995). This model was adapted to the pulsed steady-state saturation regimen, which are achieved using MRI pulse sequences, and enabled the first experimental demonstrations of MPF maps of the human brain along with the maps of other model parameters using multi-parameter voxel-wise fit of Z-spectral images (Sled and Pike, 2001; Yarnykh, 2002). Also, several methods based on the analysis of bi-exponential longitudinal relaxation were reported. The RF pulse excitation schemes in these techniques may vary and may be preferentially targeted at either the free water or macromolecular protons. Within this paradigm, the techniques based on selective inversion of free water magnetization (Gochberg and Gore, 2003, 2007; Dortch et al., 2011; Cronin et al., 2020), stimulated echo preparation (Ropele et al., 2003; Soellinger et al., 2011), and broadband saturation of the macromolecular pool (van Gelderen et al., 2017) were developed. On-resonance saturation of water protons caused by readout RF pulses in fast gradient-echo sequences also can be used as a tool for MPF mapping (Gloor et al., 2008; Garcia et al., 2010; Bayer et al., 2021) based

on steady-state models, where the signal is sampled as a function of the excitation pulse duration and flip angle.

The two-pool model contains six independent parameters. None of existing qMT methods can simultaneously measure all of them, and certain assumptions are required. In Z-spectroscopic methods,  $T_1$  of the pools are unavailable from the model fit and are mathematically coupled with cross-relaxation parameters. Accordingly, separate  $T_1$  mapping is usually performed, and  $T_1$  of the free water pool ( $T_1^F$ ) is calculated under some assumption about  $T_1$  of the macromolecular pool ( $T_1^M$ ). The common assumptions include equating them (Yarnykh, 2002) or setting  $T_1^M = 1$  s (Morrison and Henkelman, 1995).  $T_1$  measurements also may need to be corrected for the cross-relaxation effect (Mossahebi et al., 2014). In cross-relaxometric experiments,  $T_2$  of the pools cannot be extracted from data and are usually estimated by simulations in order to approximate the initial magnetization state (Gochberg and Gore, 2003; Ropele et al., 2003; Gloor et al., 2008; van Gelderen et al., 2017).

Simultaneous estimation of many parameters (usually 4 or 3) in qMT techniques requires a large number of source images, which result in impractically long data acquisition (>30 min for the human whole-brain examination), particularly in earlier methods (Sled and Pike, 2001; Ramani et al., 2002; Yarnykh, 2002; Gloor et al., 2008; Dortch et al., 2011). Additional  $B_0$  and  $B_1$  maps are also frequently used for correction of errors caused by field non-uniformities (Sled and Pike, 2001; Gloor et al., 2008; Yarnykh, 2012; Boudreau et al., 2018), thus further increasing examination time. Reduction of the acquisition time can be achieved using several strategies including optimized schedules of variable experimental parameters (Cercignani and Alexander, 2006; Li et al., 2010; Levesque et al., 2011; Battiston et al., 2018; Boudreau and Pike, 2018; Cronin et al., 2020), specialized sequences enabling acquisition of several data points within a single scan (Soellinger et al., 2011; van Gelderen et al., 2017; Battiston et al., 2019), and a reduction of the model dimension by constraining certain parameters or their combinations (Ropele et al., 2003; Yarnykh and Yuan, 2004; Cercignani et al., 2005; Yarnykh, 2012). The last approach resulted in the most radical solution providing MPF estimation from a single spoiled gradient-echo image with off-resonance saturation (Yarnykh, 2012) and a  $T_1$  map calculated using the two-point variable flip angle method (Deoni et al., 2005). The single-point method exploits negligible variability of the cross-relaxation rate constant (in the macromolecules-to-water direction),  $T_2$  of macromolecular protons, and the product of observed  $R_1 = 1/T_1$  and  $T_2$  of the free water pool in brain tissues (Yarnykh, 2012). These quantities are fixed in the reconstruction algorithm, thus making MPF the only adjustable parameter. Further acceleration of the single-point technique included elimination of a reference image (Yarnykh, 2016), which is usually needed in most qMT techniques, exclusion of  $B_0$  mapping due to a negligible effect of  $B_0$ -related errors (Yarnykh et al., 2020), and a new data-driven algorithm for  $B_1$  non-uniformity correction (Yarnykh, 2021), which obviates commonly used in qMT protocols  $B_1$  mapping sequences. With these improvements, the entire single-point MPF mapping protocol consists of only three spoiled gradient-echo sequences

providing MT-,  $T_1$ -, and proton-density-weighted images. Acceleration achieved with the single-point MPF mapping method can be converted into either high-resolution acquisition with a generally acceptable for human neuroscience applications scan time (about 15 min for a whole-brain dataset with isotropic 1.25 mm<sup>3</sup> resolution; Yarnykh, 2021) or fast clinically targeted protocols (3.5 min for a whole-brain dataset with 1.5 × 1.5 × 5.0 mm<sup>3</sup> resolution; Yarnykh et al., 2018b). Due to lesser sensitivity to noise, single-point MPF mapping showed improved reproducibility compared to multi-parameter techniques. Particularly, reported coefficients of variation of repeated measurements in the human brain were 1–2% for the single-point method (Yarnykh et al., 2020; Smirnova et al., 2021) and about 5% for multi-parameter qMT (Davies et al., 2004; Levesque et al., 2010b).

Software availability is an important aspect of future MPF mapping applications. While most studies to date utilized custom-written software tools, we identified two open-source freely available software packages enabling MPF map reconstruction. Quantitative MRI analysis MATLAB (MathWorks, Inc.; Natick, MA, United States) library “qMRLab” (Karakuzu et al., 2020; qMRLab, 2021) allows MPF map reconstruction based on several widely used multi-parameter qMT fit models (Sled and Pike, 2001; Gloor et al., 2008; Li et al., 2010). Specifically targeted at the single-point method (Yarnykh, 2012, 2016) C++ language software “MPF\_map” is available from the website (Macromolecular Proton Fraction [MPF], 2022).

## Validation in Animal Models

Macromolecular proton fraction measurements were compared with histological myelin assessment in a variety of animal models including normal animal brain (Underhill et al., 2011; Khodanovich et al., 2017) and spinal cord (Dula et al., 2010), cuprizone-induced demyelination in mice (Thiessen et al., 2013; Turati et al., 2015; Khodanovich et al., 2017, 2019; Soustelle et al., 2019, 2021), experimental autoimmune encephalomyelitis in rats (Rausch et al., 2009), lipopolysaccharide-induced focal demyelination in rats (Janve et al., 2013), hexachlorophene-induced intramyelinic edema in rats (Harkins et al., 2013), genetic hypomyelination (Ou et al., 2009a,b; West et al., 2018) and hypermyelination (West et al., 2018) in mice, ischemic stroke in rats (Khodanovich et al., 2018, 2021), spinal cord injury in primates (Wang et al., 2016, 2019; Wu et al., 2020), and demyelinated peripheral nerve *ex vivo* (Odrobina et al., 2005; Ou et al., 2009a). All studies reported qualitative correspondence of demyelinated anatomical zones with a reduced MPF and/or MPF reduction associated with demyelination relative to a control sample. When histology was quantitatively assessed, MPF demonstrated strong correlations with histological myelin markers characterized by correlation coefficients in a range 0.7–0.99 (Underhill et al., 2011; Janve et al., 2013; Thiessen et al., 2013; Turati et al., 2015; Khodanovich et al., 2017, 2018, 2019, 2021; West et al., 2018; Soustelle et al., 2019, 2021).

Several works focused on validation of MPF as a tool for monitoring re-myelination that is of critical importance for therapeutic intervention studies. An increase in MPF was correlated with re-myelination after withdrawal of cuprizone

**TABLE 1** | Summary of MPF applications in human conditions other than multiple sclerosis (MS).

Condition	Measurement technique	Main findings
Alzheimer's disease (AD)	Multipoint off-resonance (Ridha et al., 2007; Kiefer et al., 2009; Giulietti et al., 2012).	Decreased hippocampal combined index $MPF/[(1 - MPF)R_1]$ (Ridha et al., 2007). Increased hippocampal MPF (Kiefer et al., 2009). No significant effect on MPF according to voxel-based analysis but a reduced forward exchange rate constant in multiple cortical regions (Giulietti et al., 2012).
Genetic risk variants of AD	Multipoint off-resonance (Mole et al., 2020a,b).	Reduced MPF in the right parahippocampal cingulum (Mole et al., 2020a) and left thalamus (Mole et al., 2020b) in participants with APOE-ε4 genetic risk factor and family history of AD.
Interferon-α induced fatigue	Steady-state multipoint on-resonance (Dowell et al., 2016).	No significant effect on MPF according to voxel-based analysis but an increased forward exchange rate constant in the striatum and insula (Dowell et al., 2016).
Huntington's disease	Multipoint off-resonance (Bourbon-Teles et al., 2019; Casella et al., 2020).	MPF decrease in whole-brain WM (Bourbon-Teles et al., 2019; Casella et al., 2020). Motor training induced a significant MPF increase in the corpus callosum and motor pathways (Casella et al., 2020).
Mild traumatic brain injury	Single-point (Petrie et al., 2014).	Significant MPF reduction in whole-brain WM and GM (Petrie et al., 2014).
Normal aging	Multipoint off-resonance (Metzler-Baddeley et al., 2019b; Coad et al., 2020; Mole et al., 2020a).	Significant negative correlations between MPF and age in the fornix (Metzler-Baddeley et al., 2019b; Coad et al., 2020) and whole-brain WM (Mole et al., 2020a).
Obesity	Multipoint off-resonance (Metzler-Baddeley et al., 2019a).	MPF in the fornix negatively correlated with markers of obesity (Metzler-Baddeley et al., 2019a).
Brain tumors	Multipoint off-resonance (Yarnykh, 2002; Tozer et al., 2011; Mehrabian et al., 2018a,b); steady-state multipoint on-resonance (Garcia et al., 2015); single-point (Korostyshevskaya et al., 2018).	Variable MPF decrease relative to normal WM in all studied tumors including gliomas (Yarnykh, 2002; Tozer et al., 2011; Garcia et al., 2015; Mehrabian et al., 2018a,b), meningiomas (Garcia et al., 2015), and brain metastases (Garcia et al., 2015). Increased MPF relative to fetal brain tissue in fetal collagen-rich medulloblastoma (Korostyshevskaya et al., 2018).
Parkinson's disease	Single-point and multipoint off-resonance (Trujillo et al., 2017b).	Increased MPF in the substantia nigra, good agreement between single- and multi-point techniques (Trujillo et al., 2017b).
Adrenomyeloneuropathy	Multipoint off-resonance (Smith et al., 2009).	Significantly decreased MPF in the dorsal column of the spinal cord with no differences in the lateral columns and GM (Smith et al., 2009).
Fabry disease	Multipoint off-resonance (Underhill et al., 2015).	MPF reduction in left posterior brain WM, which was negatively associated with age (Underhill et al., 2015).
Myotonic dystrophy type 1	Multipoint off-resonance (Leddy et al., 2021).	Reduced MPF in WM lesions, no differences between patients and controls in NAWM (Leddy et al., 2021).
Schizophrenia	Multipoint off-resonance (Kiefer et al., 2004; Kalus et al., 2005); single-point (Smirnova et al., 2021; Sui et al., 2021).	No significant effect on MPF in the hippocampus (Kiefer et al., 2004) and amygdala (Kalus et al., 2005). Significant MPF decrease in whole-brain WM and GM associated with negative symptoms. Significant negative correlation between MPF in WM and disease duration (Smirnova et al., 2021). Voxel-based patterns of variable increase and decrease in cortical MPF depending on the disease duration. Geometric non-linearity of the cortical MPF profile decreased in patients and negatively correlated with disease duration (Sui et al., 2021).
Small vessel disease (white matter hyperintensities)	Non-conventional estimation as $MT\ ratio/T_1$ (Iordanishvili et al., 2019).	Decreased MPF in WM hyperintensities. Periventricular hyperintensities had lower MPF than deep WM ones. A decrease in MPF corresponds to lesion severity according to Fazekas scale (Iordanishvili et al., 2019).
Systemic inflammation	Steady-state multipoint on-resonance (Harrison et al., 2015).	No significant effect on MPF according to voxel-based analysis but an increased forward exchange rate constant in the insula (Harrison et al., 2015).

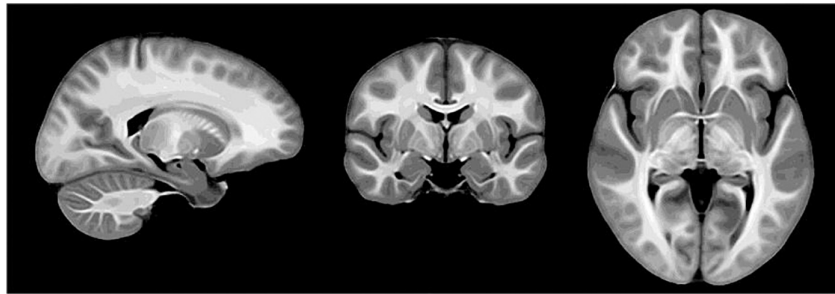


**FIGURE 1** | Study-specific template derived from macromolecular proton fraction (MPF) maps of 146 adolescent study subjects (reprinted from Corrigan et al. (2021); free PMC article).

(Turati et al., 2015; Khodanovich et al., 2019) and replicated restoration of oligodendrogenesis (Khodanovich et al., 2019) in WM and GM of cuprizone-pretreated mice. In the stroke model, MPF showed a unique capability to identify local post-ischemic remyelination, which was unobservable with conventional imaging techniques (Khodanovich et al., 2021).

Animal studies provided important insights into specificity of MPF to myelin and a role of potential confounders. MPF in normal brain tissues is largely independent of the total cell count and axonal density (Underhill et al., 2011). The loss of axons and neurons in ischemic stroke did not affect MPF (Khodanovich et al., 2018). MPF in the ischemic infarct was also found to be insensitive to microglial (Khodanovich et al., 2018) and astroglial (Khodanovich et al., 2021) proliferation, which represent pathological hallmarks of sub-acute and chronic stroke lesions. At the same time, due to dilution of the macromolecular content, MPF is affected by edema (Stanisz et al., 2004; Harkins et al., 2013; Khodanovich et al., 2018), which may cause up to 10–15% overestimation of myelin loss by MPF in acute stroke (Khodanovich et al., 2018). Multi-modal approaches were proposed to correct the effect of water content changes on MPF, particularly using proton density (Giacomini et al., 2009; Mossahebi et al., 2015) or T<sub>2</sub> measurements (Khodanovich et al., 2018), but they need more rigorous validation.

Animal models of brain development were not studied as extensively as demyelination models. Nevertheless, several publications indicate utility of MPF for monitoring normal or abnormal myelin development (Samsonov et al., 2012; Lu et al., 2018; Goussakov et al., 2019). Using MPF, these studies demonstrated dramatic distinctions in temporal myelination trajectories between the genetic canine demyelination model and normal animals (Samsonov et al., 2012), widespread effect of ischemia-hypoxia on postnatal myelination in murine WM and GM (Goussakov et al., 2019), and alterations in age-dependent myelin development caused by microbiota in mice (Lu et al., 2018).

## Neuroscience Applications

The most common primary demyelinating disease, multiple sclerosis (MS) attracted significant interest as an area of clinical MPF applications. The earliest technical development studies (Sled and Pike, 2001; Yarnykh, 2002) demonstrated that MPF

maps clearly depict MS lesions in WM as areas of low MPF. Subsequent reports identified the capability of MPF to detect microscopic demyelination in normal-appearing WM (NAWM) (Davies et al., 2003, 2004; Tozer et al., 2003, 2005; Narayanan et al., 2006; Cercignani et al., 2009; Spano et al., 2010; Yarnykh et al., 2015, 2018a; Bagnato et al., 2020). However, some studies did not find significant NAWM MPF differences between patients and controls (Bagnato et al., 2018; McKeithan et al., 2019), probably due to methodological distinctions in acquisition protocols. MPF provided new insights into lesion pathology in MS enabling studies of demyelination heterogeneity (Levesque et al., 2005; Clarke et al., 2021) and temporal evolution (Giacomini et al., 2009; Levesque et al., 2010a). Post-mortem MPF and histology studies of MS (Schmierer et al., 2007; Bagnato et al., 2018) confirmed good agreement between demyelination and a reduced MPF. The majority of MS studies utilized multipoint techniques with either off-resonance saturation (Sled and Pike, 2001; Yarnykh, 2002; Tozer et al., 2003, 2005; Davies et al., 2003, 2004; Levesque et al., 2005; Narayanan et al., 2006; Schmierer et al., 2007; Cercignani et al., 2009; Giacomini et al., 2009; Levesque et al., 2010a; Spano et al., 2010) or selective inversion-recovery preparation (Bagnato et al., 2018, 2020; McKeithan et al., 2019; Clarke et al., 2021) to obtain MPF maps. The single-point method (Yarnykh, 2012) extended the area of MPF applications to GM (Yarnykh et al., 2015, 2018a) and demonstrated strong associations of GM MPF with MS disability scales and disease phenotype (Yarnykh et al., 2015). The single-point method was also adapted to the spinal cord imaging (Smith et al., 2014) and showed a significant reduction of both NAWM and GM MPF in MS (Smith et al., 2017).

Applications of MPF in other conditions are scarce. The summary of non-MS clinical applications of MPF and key findings is provided in **Table 1**. Collectively, these studies indicate growing usage of MPF as an exploratory myelin imaging tool in diseases not primarily related to myelin pathology and suggest that MPF mapping adds a new dimension in quantitative clinical neuroimaging.

Brain development is another promising area of MPF applications since myelination is a fundamental component of CNS maturation. Fast single-point MPF mapping was used to investigate the earliest stage of myelin development in the fetal brain and showed close correlations with gestational age

in the anatomic regions with known prenatal myelination onset (Yarnykh et al., 2018b; Korostyshevskaya et al., 2019). It was also demonstrated that the single-point method enables reliable measurements of very low MPF values in the fetal brain, which are about fivefold lower than MPF in adult WM (Yarnykh et al., 2018b; Korostyshevskaya et al., 2018, 2019). A recent large-scale study investigated spatiotemporal trajectories of protracted myelin development during adolescence using high-resolution MPF maps and identified that GM myelination is characterized by a significantly faster rate as compared to WM and correlates with puberty (Corrigan et al., 2021). In the technical aspect, MPF maps used in this study demonstrated unprecedented anatomical contrast, as illustrated by the study template in **Figure 1**.

## DISCUSSION

Substantial body of evidence confirms high sensitivity and specificity of MPF to myelin. At the same time, early brain development (pre- or postnatal) remains an area where animal model studies could provide an important background for future clinical applications. Water content alterations remain a sole major confounder of MPF according to prior studies. Development of multimodal imaging approaches to mitigate the effect of water content changes would be of crucial value for MPF application in pathological conditions involving significant edema component, such as acute stroke or brain injury. In the perspective of clinical translation, MPF mapping should enable sufficiently fast acquisition and independence of a particular imaging platform. The last requirement can be met, if a technique employs standard pulse sequences provided by most MRI equipment manufacturers. In the current state of development, only two approaches [single-point synthetic-reference method (Yarnykh, 2016) and selective inversion-recovery with optimized sampling and accelerated

acquisition (Cronin et al., 2020)] allow designs of MPF mapping protocols based on unmodified sequences and provide whole-brain acquisition in less than 10 min. Since fast MPF mapping employs constrained reconstruction algorithms, consensus is needed regarding the details of the fit procedure and values of constrained parameters to facilitate comparisons between multiple studies. This aspect may involve further model refinements, such as more accurate parameters modeling macromolecular protons (Helms and Hagberg, 2009; van Gelderen et al., 2016, 2017). Finally, multi-platform protocol harmonization and repeatability studies are needed to enable MPF applications in multicenter clinical trials.

## AUTHOR CONTRIBUTIONS

AK and AN contributed to the literature research, and manuscript drafting and formatting according to the journal guidelines. VY overviewed the general concept and design of the study and made final corrections to the manuscript. All authors contributed to the article and approved the submitted version.

## FUNDING

The authors received support from the National Institutes of Health grants R21NS109727 and R24NS104098. AK was also supported by the Russian Science Foundation project No. 21-75-00038.

## SUPPLEMENTARY MATERIAL

The Supplementary Material for this article can be found online at: <https://www.frontiersin.org/articles/10.3389/fnins.2022.819912/full#supplementary-material>

## REFERENCES

- Anisimov, N. V., Pavlova, O. S., Pirogov, Y. A., and Yarnykh, V. L. (2020). Three-dimensional fast single-point macromolecular proton fraction mapping of the human Brain at 0.5 Tesla. *Quant. Imag. Med. Surg.* 10, 1441–1449. doi: 10.21037/qims-19-1057
- Bagnato, F., Hametner, S., Franco, G., Pawate, S., Sriram, S., Lassmann, H., et al. (2018). Selective inversion recovery quantitative magnetization transfer brain MRI at 7 T: clinical and postmortem validation in multiple sclerosis. *J. Neuroimag.* 28, 380–388. doi: 10.1111/jon.12511
- Bagnato, F., Franco, G., Ye, F., Fan, R., Commiskey, P., Smith, S. A., et al. (2020). Selective inversion recovery quantitative magnetization transfer imaging: toward a 3 T Clinical application in multiple sclerosis. *Mult. Scler.* 26, 457–467. doi: 10.1177/1352458519833018
- Battiston, M., Grussu, F., Ianus, A., Schneider, T., Prados, F., Fairney, J., et al. (2018). An optimized framework for quantitative magnetization transfer imaging of the cervical spinal cord in Vivo. *Magn. Reson. Med.* 79, 2576–2588. doi: 10.1002/mrm.26909
- Battiston, M., Schneider, T., Grussu, F., Yiannakas, M. C., Prados, F., De Angelis, F., et al. (2019). Fast bound pool fraction mapping via steady-state magnetization transfer saturation using single-shot EPI. *Magn. Reson. Med.* 82, 1025–1040. doi: 10.1002/mrm.27792
- Bayer, F. M., Bock, M., Jezzard, P., and Smith, A. K. (2021). Unbiased signal equation for quantitative magnetization transfer mapping in balanced steady-state free precession MRI. *Magn. Reson. Med.* 2021:28940. doi: 10.1002/mrm.28940
- Birkel, C., Birkel-Toegelhofer, A. M., Endmayr, V., Hoftberger, R., Kasprian, G., Krebs, C., et al. (2019). The Influence of brain iron on myelin water imaging. *Neuroimage* 199, 545–552. doi: 10.1016/j.neuroimage.2019.05.042
- Bourbon-Teles, J., Bells, S., Jones, D. K., Coulthard, E., Rosser, A., and Metzler-Baddeley, C. (2019). Myelin breakdown in human huntington's disease: multimodal evidence from diffusion MRI and Quantitative Magnetization Transfer. *Neuroscience* 403, 79–92. doi: 10.1016/j.neuroscience.2017.05.042
- Boudreau, M., and Pike, G. B. (2018). Sensitivity regularization of the cramer-rao lower bound to minimize b1 nonuniformity effects in quantitative magnetization transfer Imaging. *Magn. Reson. Med.* 80, 2560–2572. doi: 10.1002/mrm.27337
- Boudreau, M., Stikov, N., and Pike, G. B. (2018). B1-Sensitivity analysis of quantitative magnetization transfer imaging. *Magn. Reson. Med.* 79, 276–285. doi: 10.1002/mrm.26673
- Casella, C., Bourbon-Teles, J., Bells, S., Coulthard, E., Parker, G. D., Rosser, A., et al. (2020). Drumming motor sequence training induces apparent myelin remodelling in huntington's disease: a longitudinal diffusion mri and quantitative magnetization transfer Study. *J. Huntingt. Dis.* 9, 303–320. doi: 10.3233/JHD-200424

- Cercignani, M., and Alexander, D. C. (2006). Optimal acquisition schemes for in vivo quantitative magnetization Transfer MRI. *Magn. Reson. Med.* 56, 803–810. doi: 10.1002/mrm.21003
- Cercignani, M., Symms, M. R., Schmierer, K., Boulby, P. A., Tozer, D. J., Ron, M., et al. (2005). Three-Dimensional quantitative magnetisation transfer imaging of the human brain. *Neuroimage* 27, 436–441. doi: 10.1016/j.neuroimage.2005.04.031
- Cercignani, M., Basile, B., Spano, B., Comanducci, G., Fasano, F., Caltagirone, C., et al. (2009). Investigation of quantitative magnetization transfer parameters of lesions and normal appearing white matter in multiple sclerosis. *NMR Biomed.* 22, 646–653. doi: 10.1002/nbm.1379
- Clarke, M. A., Lakhani, D. A., Wen, S., Gao, S., Smith, S. A., Dortch, R., et al. (2021). Perilesional neurodegenerative injury in multiple sclerosis: relation to focal lesions and impact on disability. *Mult. Scler. Relat. Disord.* 49:102738. doi: 10.1016/j.msard.2021.102738
- Coad, B. M., Craig, E., Louch, R., Aggleton, J. P., Vann, S. D., and Metzler-Baddeley, C. (2020). Precommissural and postcommissural fornix microstructure in healthy aging and Cognition. *Brain Neurosci. Adv.* 4:99316. doi: 10.1177/2398212819899316
- Corrigan, N. M., Yarnykh, V. L., Hippe, D. S., Owen, J. P., Huber, E., Zhao, T. C., et al. (2021). Myelin development in cerebral gray and white matter during adolescence and late childhood. *Neuroimage* 227:117678. doi: 10.1016/j.neuroimage.2020.117678
- Cronin, M. J., Xu, J., Bagnato, F., Gochberg, D. F., Gore, J. C., and Dortch, R. D. (2020). Rapid whole-brain quantitative magnetization transfer imaging using 3D Selective Inversion Recovery Sequences. *Magn. Reson. Imag.* 68, 66–74. doi: 10.1016/j.mri.2020.01.014
- Davies, G. R., Ramani, A., Dalton, C. M., Tozer, D. J., Wheeler-Kingshott, C. A., Barker, G. J., et al. (2003). Preliminary magnetic resonance study of the macromolecular proton fraction in white matter: a potential marker of Myelin? *Mult. Scler.* 9, 246–249. doi: 10.1191/1352458503ms911oa
- Davies, G. R., Tozer, D. J., Cercignani, M., Ramani, A., Dalton, C. M., Thompson, A. J., et al. (2004). Estimation of the macromolecular proton fraction and bound pool T2 in Multiple Sclerosis. *Mult. Scler.* 10, 607–613. doi: 10.1191/1352458504ms1105oa
- Deoni, S. C. L., Peters, T. M., and Rutt, B. K. (2005). High-Resolution T1 and T2 Mapping of the brain in a clinically acceptable time with DESPOT1 and DESPOT2. *Magn. Reson. Med.* 53, 237–241. doi: 10.1002/mrm.20314
- Deoni, S. C. L., Rutt, B. K., Arun, T., Pierpaoli, C., and Jones, D. K. (2008). Gleaning Multicomponent T1 and T2 information from steady-state imaging data. *Magn. Reson. Med.* 60, 1372–1387. doi: 10.1002/mrm.21704
- Dortch, R. D., Li, K., Gochberg, D. F., Welch, E. B., Dula, A. N., Tamhane, A. A., et al. (2011). Quantitative magnetization transfer imaging in human brain at 3 T via Selective Inversion Recovery. *Magn. Reson. Med.* 66, 1346–1352. doi: 10.1002/mrm.22928
- Dowell, N. G., Cooper, E. A., Tibble, J., Voon, V., Critchley, H. D., Cercignani, M., et al. (2016). acute changes in striatal microstructure predict the development of interferon-Alpha Induced Fatigue. *Biol. Psychiatry* 79, 320–328. doi: 10.1016/j.biopsych.2015.05.015
- Dula, A. N., Gochberg, D. F., Valentine, H. L., Valentine, W. M., and Does, M. D. (2010). Multiexponential T2, magnetization transfer, and quantitative histology in white Matter Tracts of rat Spinal Cord. *Magn. Reson. Med.* 63, 902–909. doi: 10.1002/mrm.22267
- Duyn, J. H., and Schenck, J. (2017). Contributions to Magnetic Susceptibility of Brain Tissue. *NMR Biomed.* 30:3546. doi: 10.1002/nbm.3546
- Garcia, M., Gloor, M., Wetzel, S. G., Radue, E. W., Scheffler, K., and Bieri, O. (2010). Characterization of normal appearing brain structures using high-resolution quantitative magnetization transfer steady-state free precession imaging. *Neuroimage* 52, 532–537. doi: 10.1016/j.neuroimage.2010.04.242
- Garcia, M., Gloor, M., Bieri, O., Radue, E.-W., Lieb, J. M., Cordier, D., et al. (2015). Imaging of primary brain tumors and metastases with fast quantitative 3-dimensional Magnetization Transfer. *J. Neuroimag.* 25, 1007–1014. doi: 10.1111/jon.12222
- Giacomini, P. S., Levesque, I. R., Ribeiro, L., Narayanan, S., Francis, S. J., Pike, G. B., et al. (2009). Measuring demyelination and remyelination in acute multiple sclerosis lesion Voxels. *Arch. Neurol.* 66, 375–381. doi: 10.1001/archneurol.2008.578
- Giulietti, G., Bozzali, M., Figura, V., Spanò, B., Perri, R., Marra, C., et al. (2012). Quantitative magnetization transfer provides information complementary to grey matter atrophy in alzheimer's Disease Brains. *Neuroimage* 59, 1114–1122. doi: 10.1016/j.neuroimage.2011.09.043
- Gloor, M., Scheffler, K., and Bieri, O. (2008). Quantitative magnetization transfer imaging using balanced SSFP. *Magn. Reson. Med.* 60, 691–700. doi: 10.1002/mrm.21705
- Gochberg, D., and Gore, J. (2003). Quantitative imaging of magnetization transfer using an inversion recovery sequence. *Magn. Reson. Med.* 49, 501–505. doi: 10.1002/mrm.10386
- Gochberg, D., and Gore, J. (2007). Quantitative magnetization transfer imaging via selective inversion recovery with short repetition Times. *Magn. Reson. Med.* 57, 437–441. doi: 10.1002/mrm.21143
- Goussakov, I., Synowiec, S., Yarnykh, V., and Drobyshevsky, A. (2019). Immediate and delayed decrease of long term potentiation and memory deficits after neonatal intermittent Hypoxia. *Int. J. Dev. Neurosci.* 74, 27–37. doi: 10.1016/j.ijdevneu.2019.03.001
- Harkins, K. D., Valentine, W. M., Gochberg, D. F., and Does, M. D. (2013). In-Vivo Multi-Exponential T2, magnetization transfer and quantitative histology in a rat model of intramyelinic Edema. *Neuroimage Clin.* 2, 810–817. doi: 10.1016/j.nicl.2013.06.007
- Harrison, N. A., Cooper, E., Dowell, N. G., Keramida, G., Voon, V., Critchley, H. D., et al. (2015). Quantitative magnetization transfer imaging as a biomarker for effects of systemic Inflammation on the Brain. *Biol. Psychiatry* 78, 49–57. doi: 10.1016/j.biopsych.2014.09.023
- Heath, F., Hurley, S. A., Johansen-Berg, H., and Sampaio-Baptista, C. (2018). Advances in Noninvasive Myelin Imaging. *Dev. Neurobiol.* 78, 136–151. doi: 10.1002/dneu.22552
- Helms, G., and Hagberg, G. E. (2009). In Vivo quantification of the bound pool T1 in human white matter using the binary spin-bath model of progressive magnetization transfer Saturation. *Phys. Med. Biol.* 54, N529–N540. doi: 10.1088/0031-9155/54/23/N01
- Henkelman, R. M., Stanisz, G. J., and Graham, S. J. (2001). Magnetization Transfer in MRI: a Review. *NMR Biomed.* 14, 57–64. doi: 10.1002/nbm.683
- Hwang, D., Kim, D.-H., and Du, Y. P. (2010). In Vivo multi-slice mapping of myelin water Content Using T2\* Decay. *Neuroimage* 52, 198–204. doi: 10.1016/j.neuroimage.2010.04.023
- Iordanishvili, E., Schall, M., Loução, R., Zimmermann, M., Kotetishvili, K., Shah, N. J., et al. (2019). Quantitative MRI of cerebral white matter hyperintensities: a new approach towards understanding the underlying pathology. *Neuroimage* 202:116077. doi: 10.1016/j.neuroimage.2019.116077
- Janve, V. A., Zu, Z., Yao, S. Y., Li, K., Zhang, F. L., Wilson, K. J., et al. (2013). The Radial Diffusivity and magnetization transfer pool size ratio are sensitive markers for demyelination in a rat model of Type III Multiple Sclerosis (MS) Lesions. *Neuroimage* 74, 298–305. doi: 10.1016/j.neuroimage.2013.02.034
- Karakuzu, A., Boudreau, M., Duval, T., Boshkovski, T., Leppert, I. R., and Cabana, J. F. (2020). qMRLab: Quantitative MRI Analysis, under one Umbrella. *J. Open Sour. Softw.* 5:2343. doi: 10.21105/joss.02343
- Kalus, P., Slotboom, J., Gallinat, J., Wiest, R., Ozdoba, C., Federspiel, A., et al. (2005). The Amygdala in schizophrenia: a trimodal magnetic resonance imaging Study. *Neurosci. Lett.* 375, 151–156. doi: 10.1016/j.neulet.2004.11.004
- Khodanovich, M. Y., Sorokina, I. V., Glazacheva, V. Y., Akulov, A. E., Nemirovich-Danchenko, N. M., Romashchenko, A. V., et al. (2017). Histological validation of fast macromolecular proton fraction mapping as a quantitative myelin imaging method in the cuprizone demyelination Model. *Sci. Rep.* 7:46686. doi: 10.1038/srep46686
- Khodanovich, M. Y., Kisel, A. A., Akulov, A. E., Atochin, D. N., Kudabaeva, M. S., Glazacheva, V. Y., et al. (2018). Quantitative assessment of demyelination in ischemic stroke in vivo using macromolecular proton fraction Mapping. *J. Cereb. Blood Flow Metab.* 38, 919–931. doi: 10.1177/0271678X18755203
- Khodanovich, M., Pishchelko, A., Glazacheva, V., Pan, E., Akulov, A., Svetlik, M., et al. (2019). Quantitative imaging of white and gray matter myelination in the cuprizone demyelination model using the macromolecular proton fraction. *Cells* 8:1204. doi: 10.3390/cells8101204
- Khodanovich, M. Y., Gubskiy, I. L., Kudabaeva, M. S., Namestnikova, D. D., Kisel, A. A., Anan'ina, T. V., et al. (2021). Long-term monitoring of chronic demyelination and remyelination in a rat ischemic stroke model using

- macromolecular proton fraction Mapping. *J. Cereb. Blood Flow Metab.* 41, 2856–2869. doi: 10.1177/0271678X211020860
- Kiefer, C., Slotboom, J., Buri, C., Gralla, J., Remonda, L., Dierks, T., et al. (2004). Differentiating hippocampal subregions by means of quantitative magnetization transfer and relaxometry: preliminary Results. *Neuroimage* 23, 1093–1099. doi: 10.1016/j.neuroimage.2004.07.066
- Kiefer, C., Brockhaus, L., Cattapan-Ludewig, K., Ballinari, P., Burren, Y., Schroth, G., et al. (2009). Multi-Parametric classification of alzheimer's disease and mild cognitive impairment: the impact of quantitative magnetization transfer MR Imaging. *Neuroimage* 48, 657–667. doi: 10.1016/j.neuroimage.2009.07.005
- Korostyshevskaya, A. M., Savelov, A. A., Papusha, L. I., Druy, A. E., and Yarnykh, V. L. (2018). Congenital medulloblastoma: fetal and postnatal longitudinal observation with Quantitative MRI. *Clin. Imag.* 52, 172–176. doi: 10.1016/j.clinimag.2018.06.001
- Korostyshevskaya, A. M., Prihodko, I., Savelov, A. A., and Yarnykh, V. L. (2019). Direct comparison between apparent diffusion coefficient and macromolecular proton fraction as quantitative biomarkers of the human Fetal Brain Maturation. *J. Magn. Reson. Imag.* 50, 52–61. doi: 10.1002/jmri.26635
- Lazari, A., and Lipp, I. (2021). Can MRI measure myelin? systematic review, qualitative assessment, and meta-analysis of studies validating microstructural imaging with myelin Histology. *Neuroimage* 230:117744. doi: 10.1016/j.neuroimage.2021.117744
- Leddy, S., Serra, L., Esposito, D., Vizzotto, C., Giulietti, G., Silvestri, G., et al. (2021). Lesion distribution and substrate of white matter damage in myotonic dystrophy type 1: comparison with Multiple Sclerosis. *Neuroimag. Clin.* 29:102562. doi: 10.1016/j.nicl.2021.102562
- Levesque, I., Sled, J. G., Narayanan, S., Santos, A. C., Brass, S. D., Francis, S. J., et al. (2005). The role of edema and demyelination in chronic T1 Black Holes: a Quantitative Magnetization Transfer Study. *J. Magn. Reson. Imag.* 21, 103–110. doi: 10.1002/jmri.20231
- Levesque, I. R., Giacomini, P. S., Narayanan, S., Ribeiro, L. T., Sled, J. G., Arnold, D. L., et al. (2010a). quantitative magnetization transfer and myelin water imaging of the evolution of Acute Multiple Sclerosis Lesions. *Magn. Reson. Med.* 63, 633–640. doi: 10.1002/mrm.22244
- Levesque, I. R., Sled, J. G., Narayanan, S., Giacomini, P. S., Ribeiro, L. T., Arnold, D. L., et al. (2010b). Reproducibility of quantitative magnetization-transfer imaging parameters from repeated measurements. *Magn. Reson. Med.* 64, 391–400. doi: 10.1002/mrm.22350
- Levesque, I. R., Sled, J. G., and Pike, G. B. (2011). Iterative optimization method for design of quantitative magnetization transfer imaging experiments. *Magn. Reson. Med.* 66, 635–643. doi: 10.1002/mrm.23071
- Li, K., Zu, Z., Xu, J., Janve, V. A., Gore, J. C., Does, M. D., et al. (2010). Optimized inversion recovery sequences for quantitative t1 and magnetization transfer imaging. *Magn. Reson. Med.* 64, 491–500. doi: 10.1002/mrm.22440
- Li, K., Li, H., Zhang, X. Y., Stokes, A. M., Jiang, X., Kang, H., et al. (2016). Influence of water compartmentation and heterogeneous relaxation on quantitative magnetization transfer imaging in rodent Brain Tumors. *Magn. Reson. Med.* 76, 635–644. doi: 10.1002/mrm.25893
- Lu, J., Synowiec, S., Lu, L., Yu, Y., Bretherick, T., Takada, S., et al. (2018). Microbiota influence the development of the brain and behaviors in C57BL/6J Mice. *PLoS One* 13:e0201829. doi: 10.1371/journal.pone.0201829
- MacKay, A., Whittall, K., Adler, J., Li, D., Paty, D., and Graeb, D. (1994). In Vivo visualization of myelin water in brain by magnetic resonance. *Magn. Reson. Med.* 31, 673–677. doi: 10.1002/mrm.1910310614
- Macromolecular Proton Fraction [MPF] (2022). *Quantitative Myelin Mapping Technique for Neuroscience*. Available online at: <https://www.macromolecularmri.org> (Accessed January 13, 2022)
- Mancini, M., Karakuzu, A., Cohen-Adad, J., Cercignani, M., Nichols, T. E., and Stikov, N. (2020). An Interactive Meta-Analysis of MRI Biomarkers of Myelin. *Elife* 9:e61523. doi: 10.7554/eLife.61523
- McKeithan, L. J., Lyttle, B. D., Box, B. A., O'Grady, K. P., Dortch, R. D., Conrad, B. N., et al. (2019). 7 T Quantitative Magnetization Transfer (qMT) of cortical gray matter in multiple sclerosis correlates with cognitive impairment. *Neuroimage* 203:116190. doi: 10.1016/j.neuroimage.2019.116190
- Mehrabian, H., Lam, W. W., Myrehaug, S., Sahgal, A., and Stanis, G. J. (2018a). Glioblastoma (GBM) Effects on Quantitative MRI of Contralateral Normal Appearing White Matter. *J. Neurooncol.* 139, 97–106. doi: 10.1007/s11060-018-2846-0
- Mehrabian, H., Myrehaug, S., Soliman, H., Sahgal, A., and Stanis, G. J. (2018b). Quantitative magnetization transfer in monitoring glioblastoma (GBM) Response to Therapy. *Sci. Rep.* 8:2475. doi: 10.1038/s41598-018-20624-6
- Metzler-Baddeley, C., Mole, J. P., Leonaviciute, E., Sims, R., Kidd, E. J., and Ertefai, B. (2019a). Sex-specific effects of central adiposity and inflammatory markers on limbic Microstructure. *Neuroimage* 189, 793–803. doi: 10.1016/j.neuroimage.2019.02.007
- Metzler-Baddeley, C., Mole, J. P., Sims, R., Fasano, F., Evans, J., Jones, D. K., et al. (2019b). Fornix white matter glia damage causes hippocampal gray matter damage during age-dependent Limbic Decline. *Sci. Rep.* 9:1060. doi: 10.1038/s41598-018-37658-5
- Mole, J. P., Fasano, F., Evans, J., Sims, R., Hamilton, D. A., Kidd, E., et al. (2020a). Genetic risk of dementia modifies obesity effects on white matter myelin in cognitively healthy adults. *Neurobiol. Aging* 94, 298–310. doi: 10.1016/j.neurobiolaging.2020.06.014
- Mole, J. P., Fasano, F., Evans, J., Sims, R., Kidd, E., Aggleton, J. P., et al. (2020b). APOE-ε4-Related differences in left thalamic microstructure in cognitively healthy Adults. *Sci. Rep.* 10:19787. doi: 10.1038/s41598-020-75992-9
- Morrison, C., and Henkelman, R. M. (1995). A model for magnetization transfer in tissues. *Magn. Reson. Med.* 33, 475–482. doi: 10.1002/mrm.1910330404
- Mossahebi, P., Yarnykh, V. L., and Samsonov, A. (2014). Analysis and Correction of Biases in Cross-Relaxation MRI due to Biexponential Longitudinal Relaxation. *Magn. Reson. Med.* 71, 830–838. doi: 10.1002/mrm.24677
- Mossahebi, P., Alexander, A. L., Field, A. S., and Samsonov, A. A. (2015). Removal of cerebrospinal fluid partial volume effects in quantitative magnetization transfer imaging using a three-pool model with nonexchanging water component. *Magn. Reson. Med.* 74, 1317–1326. doi: 10.1002/mrm.25516
- Narayanan, S., Francis, S. J., Sled, J. G., Santos, A. C., Antel, S., Levesque, I., et al. (2006). Axonal injury in the cerebral normal-appearing white matter of patients with multiple sclerosis is related to concurrent demyelination in lesions but not to concurrent demyelination in normal-appearing white matter. *Neuroimage* 29, 637–642. doi: 10.1016/j.neuroimage.2005.07.017
- Naumova, A. V., Akulov, A. E., Khodanovich, M. Y., and Yarnykh, V. L. (2017). High-resolution three-dimensional macromolecular proton fraction mapping for quantitative neuroanatomical imaging of the rodent brain in ultra-high magnetic Fields. *Neuroimage* 147, 985–993. doi: 10.1016/j.neuroimage.2016.09.036
- Odrobina, E., Lam, T., Pun, T., Midha, R., and Stanis, G. (2005). MR Properties of Excised Neural Tissue Following Experimentally Induced Demyelination. *NMR Biomed.* 18, 277–284. doi: 10.1002/nbm.951
- Ou, X., Sun, S. W., Liang, H. F., Song, S. K., and Gochberg, D. F. (2009a). Quantitative magnetization transfer measured pool-size ratio reflects optic nerve myelin content in Ex Vivo Mice. *Magn. Reson. Med.* 61, 364–371. doi: 10.1002/mrm.21850
- Ou, X., Sun, S. W., Liang, H. F., Song, S. K., and Gochberg, D. F. (2009b). The MT Pool Size Ratio and the DTI Radial diffusivity may reflect the myelination in shiverer and Control Mice. *NMR Biomed.* 22, 480–487. doi: 10.1002/nbm.1358
- Petrie, E. C., Cross, D. J., Yarnykh, V. L., Richards, T., Martin, N. M., Pagulayan, K., et al. (2014). Neuroimaging, behavioral, and psychological sequelae of repetitive combined blast/impact mild traumatic brain injury in iraq and afghanistan war Veterans. *J. Neurotrauma* 31, 425–436. doi: 10.1089/neu.2013.2952
- Piredda, G. F., Hilbert, T., Thiran, J. P., and Kober, T. (2021). Probing Myelin Content of the Human Brain with MRI: a Review. *Magn. Reson. Med.* 85, 627–652. doi: 10.1002/mrm.28509
- qMRLab (2021). *Quantitative MRI. Under one Umbrella*. Available online at: <http://qmrlab.org> (Accessed January 13, 2022)
- Ramani, A., Dalton, C., Miller, D. H., Tofts, P. S., and Barker, G. J. (2002). Precise Estimate of Fundamental In-Vivo MT parameters in human brain in clinically feasible times. *Magn. Reson. Imag.* 20, 721–731. doi: 10.1016/s0730-725x(02)00598-2
- Rausch, M., Tofts, P. S., Lervik, P., Walmsley, A. R., Mir, A., Schubart, A., et al. (2009). Characterization of white matter damage in animal models of multiple sclerosis by magnetization transfer ratio and quantitative mapping of the apparent bound proton Fraction F. *Mult. Scler.* 15, 16–27. doi: 10.1177/1352458508096006
- Ridha, B. H., Tozer, D. J., Symms, M. R., Stockton, K. C., Lewis, E. B., Siddique, M. M., et al. (2007). Quantitative magnetization transfer imaging

- in Alzheimer Disease. *Radiology* 244, 832–837. doi: 10.1148/radiol.2443061128
- Ropele, S., Seifert, T., Enzinger, C., and Fazekas, F. (2003). Method for Quantitative Imaging of the Macromolecular 1H Fraction in Tissues. *Magn. Reson. Med.* 49, 864–871. doi: 10.1002/mrm.10427
- Samsonov, A., Alexander, A. L., Mossahebi, P., Wu, Y. C., Duncan, I. D., and Field, A. S. (2012). Quantitative MR imaging of two-pool magnetization transfer model parameters in myelin mutant shaking Pup. *Neuroimage* 62, 1390–1398. doi: 10.1016/j.neuroimage.2012.05.077
- Schmierer, K., Tozer, D. J., Scaravilli, F., Altmann, D. R., Barker, G. J., Tofts, P. S., et al. (2007). Quantitative magnetization transfer imaging in postmortem multiple sclerosis Brain. *J. Magn. Reson. Imaging* 26, 41–51. doi: 10.1002/jmri.20984
- Sled, J. G. (2018). Modelling and interpretation of magnetization transfer imaging in the Brain. *Neuroimage* 182, 128–135. doi: 10.1016/j.neuroimage.2017.11.065
- Sled, J. G., and Pike, G. B. (2001). Quantitative imaging of magnetization transfer exchange and relaxation properties In Vivo Using MRI. *Magn. Reson. Med.* 46, 923–931. doi: 10.1002/mrm.1278
- Smirnova, L. P., Yarnykh, V. L., Parshukova, D. A., Kornetova, E. G., Semke, A. V., Usova, A. V., et al. (2021). Global hypomyelination of the brain white and gray matter in schizophrenia: quantitative imaging using macromolecular proton Fraction. *Transl. Psychiatry* 11:365. doi: 10.1038/s41398-021-01475-8
- Smith, S. A., Golay, X., Fatemi, A., Mahmood, A., Raymond, G. V., Moser, H. W., et al. (2009). Quantitative magnetization transfer characteristics of the human cervical spinal cord in vivo: application to adrenomyeloneuropathy. *Magn. Reson. Med.* 61, 22–27. doi: 10.1002/mrm.21827
- Smith, A. K., Dortch, R. D., Dethrage, L. M., and Smith, S. A. (2014). Rapid, High-resolution quantitative magnetization transfer MRI of the Human Spinal Cord. *Neuroimage* 95, 106–116. doi: 10.1016/j.neuroimage.2014.03.005
- Smith, A. K., By, S., Lyttle, B. D., Dortch, R. D., Box, B. A., Mckeithan, L. J., et al. (2017). Evaluating single-point quantitative magnetization transfer in the cervical spinal cord: application to multiple sclerosis. *Neuroimage Clin.* 16, 58–65. doi: 10.1016/j.nicl.2017.07.010
- Soellinger, M., Langkammer, C., Seifert-Held, T., Fazekas, F., and Ropele, S. (2011). Fast bound pool fraction mapping using stimulated Echoes. *Magn. Reson. Med.* 66, 717–724. doi: 10.1002/mrm.22846
- Song, S.-K., Sun, S.-W., Ramsbottom, M. J., Chang, C., Russell, J., and Cross, A. H. (2002). Dysmyelination Revealed through MRI as Increased Radial (but Unchanged Axial) Diffusion of Water. *Neuroimage* 17, 1429–1436. doi: 10.1006/nimg.2002.1267
- Soustelle, L., Antal, M. C., Lamy, J., Rousseau, F., Armspach, J. P., and Loureiro de Sousa, P. (2019). Correlations of Quantitative MRI Metrics with Myelin Basic Protein (MBP) Staining in a Murine Model of Demyelination. *NMR Biomed.* 32:e4116. doi: 10.1002/nbm.4116
- Soustelle, L., Antal, M. C., Lamy, J., Harsan, L. A., and Loureiro de Sousa, P. (2021). Determination of optimal parameters for 3D Single-point macromolecular proton fraction mapping at 7 t in healthy and demyelinated mouse Brain. *Magn. Reson. Med.* 85, 369–379. doi: 10.1002/mrm.28397
- Spano, B., Cercignani, M., Basile, B., Romano, S., Mannu, R., Centonze, D., et al. (2010). Multiparametric MR Investigation of the Motor pyramidal system in patients with 'Truly Benign'. *Multiple Sclerosis. Mult. Scler.* 16, 178–188. doi: 10.1177/1352458509356010
- Stanisz, G. J., Webb, S., Munro, C. A., Pun, T., and Midha, R. (2004). MR Properties of Excised neural tissue following experimentally induced inflammation. *Magn. Reson. Med.* 51, 473–479. doi: 10.1002/mrm.20008
- Stikov, N., Perry, L. M., Mezer, A., Rykhlevskaia, E., Wandell, B. A., Pauly, J. M., et al. (2011). Bound pool fractions complement diffusion measures to describe white matter micro and macrostructure. *Neuroimage* 54, 1112–1121. doi: 10.1016/j.neuroimage.2010.08.068
- Stüber, C., Morawski, M., Schäfer, A., Labadie, C., Wähnert, M., Leuze, C., et al. (2014). Myelin and iron concentration in the human brain: a quantitative study of mri contrast. *Neuroimage* 93, 95–106. doi: 10.1016/j.neuroimage.2014.02.026
- Sui, Y. V., Bertisch, H., Lee, H.-H., Storey, P., Babb, J. S., Goff, D. C., et al. (2021). Quantitative macromolecular proton fraction mapping reveals altered cortical myelin profile in schizophrenia spectrum Disorders. *Cereb. Cortex Commun.* 2:tgab015. doi: 10.1093/texcom/tgab015
- Thiessen, J. D., Zhang, Y., Zhang, H., Wang, L., Buist, R., Del Bigio, M. R., et al. (2013). Quantitative MRI and ultrastructural examination of the cuprizone mouse model of Demyelination. *NMR Biomed.* 26, 1562–1581. doi: 10.1002/nbm.2992
- Tozer, D., Ramani, A., Barker, G. J., Davies, G. R., Miller, D. H., and Tofts, P. S. (2003). Quantitative magnetization transfer mapping of bound protons in multiple sclerosis. *Magn. Reson. Med.* 50, 83–91. doi: 10.1002/mrm.10514
- Tozer, D. J., Davies, G. R., Altmann, D. R., Miller, D. H., and Tofts, P. S. (2005). Correlation of apparent myelin measures obtained in multiple sclerosis patients and controls from magnetization transfer and multicompartmental T2 analysis. *Magn. Reson. Med.* 53, 1415–1422. doi: 10.1002/mrm.20479
- Tozer, D. J., Rees, J. H., Benton, C. E., Waldman, A. D., Jager, H. R., and Tofts, P. S. (2011). Quantitative magnetisation transfer imaging in glioma: preliminary Results. *NMR Biomed.* 24, 492–498. doi: 10.1002/nbm.1614
- Trujillo, P., Summers, P. E., Ferrari, E., Zucca, F. A., Sturini, M., Mainardi, L. T., et al. (2017a). Contrast mechanisms associated with neuromelanin-MRI. *Magn. Reson. Med.* 78, 1790–1800. doi: 10.1002/mrm.26584
- Trujillo, P., Summers, P. E., Smith, A. K., Smith, S. A., Mainardi, L. T., Cerutti, S., et al. (2017b). Pool Size ratio of the substantia nigra in parkinson's disease derived from two different quantitative magnetization transfer approaches. *Neuroradiology* 59, 1251–1263. doi: 10.1007/s00234-017-1911-2
- Turati, L., Moscatelli, M., Mastropietro, A., Dowell, N. G., Zucca, I., Erbetta, A., et al. (2015). In Vivo quantitative magnetization transfer imaging correlates with histology during de- and remyelination in cuprizone-treated Mice. *NMR Biomed.* 28, 327–337. doi: 10.1002/nbm.3253
- Underhill, H. R., Yuan, C., and Yarnykh, V. L. (2009). Direct quantitative comparison between cross-relaxation imaging and diffusion tensor imaging of the human Brain at 3.0 T. *Neuroimage* 47, 1568–1578. doi: 10.1016/j.neuroimage.2009.05.075
- Underhill, H. R., Rostomily, R. C., Mikheev, A. M., Yuan, C., and Yarnykh, V. L. (2011). Fast bound pool fraction imaging of the in vivo rat brain: association with myelin content and validation in the C6 Glioma Model. *Neuroimage* 54, 2052–2065. doi: 10.1016/j.neuroimage.2010.10.065
- Underhill, H. R., Golden-Grant, K., Garrett, L. T., Uhrich, S., Zielinski, B. A., and Scott, C. R. (2015). Detecting the effects of fabry disease in the adult human brain with diffusion tensor imaging and fast bound-pool fraction imaging. *J. Magn. Reson. Imaging* 42, 1611–1622. doi: 10.1002/jmri.24952
- van der Weijden, C. W. J., García, D. V., Borra, R. J. H., Thurner, P., Meilof, J. F., van Laar, P. J., et al. (2021). Myelin Quantification with MRI: a Systematic Review of Accuracy and Reproducibility. *Neuroimage* 226:117561. doi: 10.1016/j.neuroimage.2020.117561
- van Gelderen, P., Jiang, X., and Duyn, J. H. (2016). Effects of Magnetization Transfer on T1 contrast in human brain white matter. *Neuroimage* 128, 85–95. doi: 10.1016/j.neuroimage.2015.12.032
- van Gelderen, P., Jiang, X., and Duyn, J. H. (2017). Rapid measurement of brain macromolecular proton fraction with transient saturation Transfer MRI. *Magn. Reson. Med.* 77, 2174–2185. doi: 10.1002/mrm.26304
- Wang, F., Li, K., Mishra, A., Gochberg, D., Min Chen, L., and Gore, J. C. (2016). Longitudinal assessment of spinal cord injuries in nonhuman primates with quantitative magnetization Transfer. *Magn. Reson. Med.* 75, 1685–1696. doi: 10.1002/mrm.25725
- Wang, F., Wu, T. L., Li, K., Chen, L. M., and Gore, J. C. (2019). Spatiotemporal trajectories of quantitative magnetization transfer measurements in injured spinal cord using Simplified Acquisitions. *Neuroimage Clin.* 23:101921. doi: 10.1016/j.nicl.2019.101921
- West, K. L., Kelm, N. D., Carson, R. P., Gochberg, D. F., Ess, K. C., and Does, M. D. (2018). Myelin Volume Fraction Imaging with MRI. *Neuroimage* 182, 511–521. doi: 10.1016/j.neuroimage.2016.12.067
- Wheeler-Kingshott, C. A., and Cercignani, M. (2009). About "Axial" and "Radial" Diffusivities. *Magn. Reson. Med.* 61, 1255–1260. doi: 10.1002/mrm.21965
- Wu, T. L., Byun, N. E., Wang, F., Mishra, A., Janve, V. A., Chen, L. M., et al. (2020). Longitudinal assessment of recovery after spinal cord injury with behavioral measures and diffusion, quantitative magnetization transfer and functional magnetic resonance imaging. *NMR Biomed.* 33:e4216. doi: 10.1002/nbm.4216
- Yarnykh, V. L. (2002). Pulsed Z-spectroscopic imaging of cross-relaxation parameters in tissues for human mri: theory and clinical applications. *Magn. Reson. Med.* 47, 929–939. doi: 10.1002/mrm.10120

- Yarnykh, V. L. (2012). Fast macromolecular proton fraction mapping from a single off-resonance magnetization transfer measurement. *Magn. Reson. Med.* 68, 166–178. doi: 10.1002/mrm.23224
- Yarnykh, V. L. (2016). Time-Efficient, high-resolution, whole brain three-dimensional macromolecular proton fraction mapping. *Magn. Reson. Med.* 75, 2100–2106. doi: 10.1002/mrm.25811
- Yarnykh, V. L. (2021). Data-Driven Retrospective Correction of B1 Field Inhomogeneity in Fast Macromolecular Proton Fraction and R1 Mapping. *IEEE Trans. Med. Imag.* 2021:3088258. doi: 10.1109/TMI.2021.3088258
- Yarnykh, V. L., and Yuan, C. (2004). Cross-relaxation imaging reveals detailed anatomy of white matter fiber tracts in the human Brain. *Neuroimage* 23, 409–424. doi: 10.1016/j.neuroimage.2004.04.029
- Yarnykh, V. L., Bowen, J. D., Samsonov, A., Repovic, P., Mayadev, A., Qian, P., et al. (2015). Fast whole-brain three-dimensional macromolecular proton fraction mapping in multiple Sclerosis. *Radiology* 274, 210–220. doi: 10.1148/radiol.14140528
- Yarnykh, V. L., Kisel, A. A., and Khodanovich, M. Y. (2020). Scan-Rescan Repeatability and Impact of B0 and B1 Field non-uniformity corrections in single-point whole-brain macromolecular proton fraction mapping. *J. Magn. Reson. Imaging* 51, 1789–1798. doi: 10.1002/jmri.26998
- Yarnykh, V. L., Krutenkova, E. P., Aitmagambetova, G., Repovic, P., Mayadev, A., Qian, P., et al. (2018a). Iron-Insensitive quantitative assessment of subcortical gray matter demyelination in multiple sclerosis using the macromolecular proton fraction. *AJNR Am. J. Neuroradiol.* 39, 618–625. doi: 10.3174/ajnr.A5542
- Yarnykh, V. L., Prihod'ko, I. Y., Savelov, A. A., and Korostyshevskaya, A. M. (2018b). Quantitative assessment of normal fetal brain myelination using fast macromolecular proton fraction mapping. *AJNR Am J Neuroradiol.* 39, 1341–1348. doi: 10.3174/ajnr.A5668
- Conflict of Interest:** The authors declare that the research was conducted in the absence of any commercial or financial relationships that could be construed as a potential conflict of interest.
- Publisher's Note:** All claims expressed in this article are solely those of the authors and do not necessarily represent those of their affiliated organizations, or those of the publisher, the editors and the reviewers. Any product that may be evaluated in this article, or claim that may be made by its manufacturer, is not guaranteed or endorsed by the publisher.
- Copyright © 2022 Kisel, Naumova and Yarnykh. This is an open-access article distributed under the terms of the Creative Commons Attribution License (CC BY). The use, distribution or reproduction in other forums is permitted, provided the original author(s) and the copyright owner(s) are credited and that the original publication in this journal is cited, in accordance with accepted academic practice. No use, distribution or reproduction is permitted which does not comply with these terms.